Absence of antiferromagnetic correlations in YNi_2B_2C

B. J. Suh, F. Borsa,* D. R. Torgeson, B. K. Cho,† P. C. Canfield, D. C. Johnston, J. Y. Rhee,‡ and B. N. Harmon
Ames Laboratory and Department of Physics and Astronomy, Iowa State University, Ames, Iowa 50011
(Received 22 November 1995)

The normal-state magnetic and electronic properties of YNi_2B_2C single crystals have been investigated by detailed ^{11}B NMR and magnetic-susceptibility measurements. The data are found to be consistent with band theory, with no evidence of Ni local magnetic moments or antiferromagnetic correlations.

The RNi_2B_2C compounds[1] have aroused great interest due to their high superconducting transition temperatures T_c compared with most other intermetallic compounds (e.g., $T_c = 16.6$ K for $R =$ Lu and 15.5 K for $R =$ Y), to the presence of a layered lattice of Ni perpendicular to the tetragonal c axis,[2] where Ni in its elemental form is an itinerant ferromagnet, and to the observation of superconductivity in compounds containing magnetic rare-earth R elements. The structure[2] is qualitatively similar to those of the layered cuprate high-T_c superconductors. However, electronic band-structure calculations[3–7] predict that the RNi_2B_2C compounds are three-dimensional d-band metals and that the superconductivity can arise from the conventional electron-phonon mechanism.

A pressing issue with regard to the mechanism for superconductivity in the RNi_2B_2C compounds is whether the Ni layers exhibit antiferromagnetic (AF) spin correlations as found in the layered cuprates. Previous ^{11}B nuclear magnetic resonance (NMR) investigations on *powders*[8–11] have suggested the occurrence of AF correlations in YNi_2B_2C and $LuNi_2B_2C$. This inference was based on a factor of ~ 2 decrease in $1/T_1T$ observed upon increasing temperature T from 20 to 300 K, where $1/T_1$ is the ^{11}B nuclear spin-lattice relaxation rate (NSLR), and/or on a nonlinear variation of $1/T_1T$ with the square of the Knight shift K.[9] For a simple metal, the magnetic susceptibility χ, $1/T_1T$ and K are each independent of T. However, the Korringa relation $1/T_1T \propto K^2$ generally describes the NSLR due to interaction of the nuclear spins with conduction-electron spins in metals, even when $1/T_1T$ and K depend on T. In this paper we report a detailed investigation of the normal state ^{11}B NMR and χ on *single crystals* of YNi_2B_2C. The use of single crystals is found to be crucial to obtaining precise and accurate data. We first show that the $\chi(T)$ data are consistent with the predictions of band theory. We then show that although $1/T_1T$ is found to decrease with T as reported before, this decrease arises from a corresponding decrease in K. On the basis of the combined χ and NMR data and comparisons with band theory predictions, we conclude that there are no observable local magnetic moments or AF spin correlations on the Ni sublattice.

Single crystals of YNi_2B_2C with $T_c = 15$ K were grown using the Ames Laboratory Ni_2B flux growth method as described previously.[12] Magnetization M measurements were carried out using a Quantum Design superconducting quantum interference device magnetometer in applied magnetic fields H up to 5 T. The contribution of ferromagnetic impurities to M, determined from $M(H)$ isotherms, was found to be equivalent to that of $\approx$ 6 at. ppm of iron metal with respect to Ni and is corrected for in Fig. 1(a) below. ^{11}B ($I = 3/2$) NMR measurements were performed with a pulse Fourier transform spectrometer at $H = 8.2$ T (112 MHz) on a c-axis-aligned stack of 12 crystals of total dimensions $\cong 10 \times 4 \times 1$ mm^3. The NMR shifts of the central line ($I_z = +\frac{1}{2} \leftrightarrow -\frac{1}{2}$) were measured with respect to H_3BO_3 aqueous solution. The NSLR was measured by saturating the central line with a single pulse and by fitting the recovery of the nuclear magnetization to the theoretical expression expected[8,11] from the solution of the master equations. The measured quantity is $T_1^{-1} = 2W$ where W is the relaxation transition probability for a change of azimuthal quantum

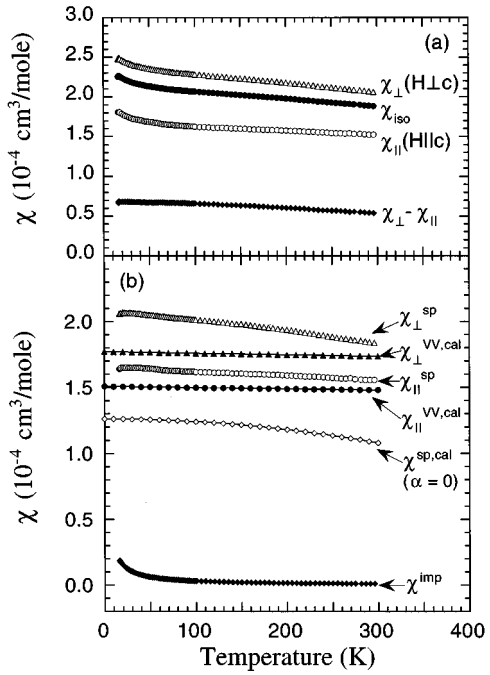

FIG. 1. (a) Magnetic susceptibility χ versus temperature T for single-crystal YNi_2B_2C. The isotropic component $\chi_{iso} \equiv (\chi_\parallel + 2\chi_\perp)/3$ and the axial component χ_{ax} given by $-3\chi_{ax} \equiv \chi_\perp - \chi_\parallel$, are as indicated. (b) The spin χ^{sp} and paramagnetic impurity χ^{imp} contributions to χ (see text). The Van Vleck $\chi^{VV,cal}$ and bare ($\alpha = 0$) isotropic spin $\chi^{sp,cal}$ susceptibilities calculated from the band structure are also shown. Note that the ordinate scales are different in (a) and (b).

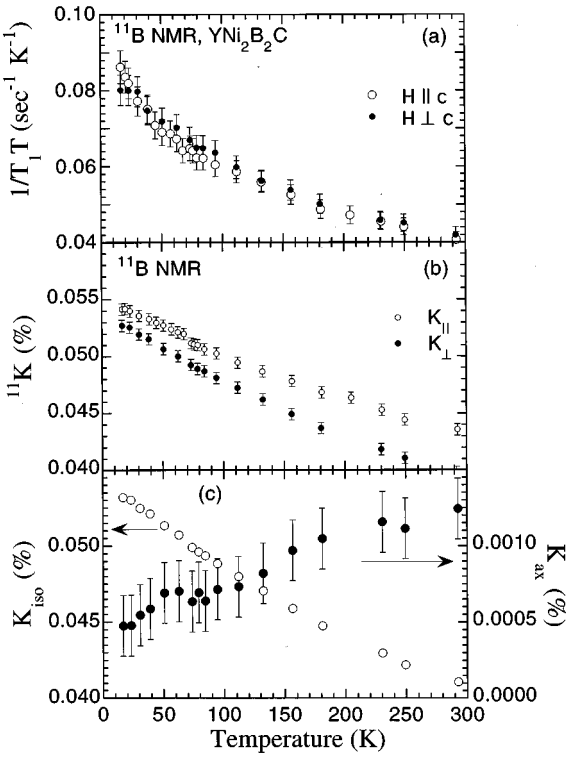

FIG. 2. ^{11}B NMR results vs T for single crystals of YNi_2B_2C: (a) $1/T_1T$, where $1/T_1$ is the nuclear spin-lattice relaxation rate, (b) Knight shift components $^{11}K_{\|}(\boldsymbol{H}\|c)$ and $^{11}K_{\perp}(\boldsymbol{H}\perp c)$ of the central line, and (c) $^{11}K_{\rm iso}\equiv(K_{\|}+2K_{\perp})/3$ and $^{11}K_{\rm ax}\equiv(K_{\|}-K_{\perp})/3$.

number of the nuclear Zeeman levels $\Delta m=\pm 1$.[11] The ^{11}B NMR spectra gave sharp (full width at half maximum $\approx$6 kHz at 300 K) central and satellite ($\pm\frac{3}{2}\leftrightarrow\pm\frac{1}{2}$) transitions for both $\boldsymbol{H}\|c$ and $\boldsymbol{H}\perp c$. From the separation of the satellite transitions, the nuclear electric quadrupole frequency is found to be constant from 300 down to 15 K [$\nu_Q=e^2qQ/2h=(698\pm1)$ kHz], indicating the absence of structural changes in this T range. The sharpness of the lines indicates that the crystals are free of structural defects and that the c-axis alignment of the different crystals in the stack is very good.

The $\chi(T)$ data for both $\boldsymbol{H}\|c$ ($\chi_{\|}$) and $\boldsymbol{H}\perp c$ ($\chi_{\perp}$) are shown in Fig. 1(a). The main features are the existence of a T-dependent anisotropic component, $-3\chi_{\rm ax}\equiv\chi_{\perp}-\chi_{\|}$, and the decrease with T of the isotropic component $\chi_{\rm iso}\equiv(\chi_{\|}+2\chi_{\perp})/3$. A T-dependent χ is often observed for narrow d-band metals.[13] A weak increase below $\sim$ 50 K is observed for $\chi_{\rm iso}$ but not for $\chi_{\rm ax}$, attributed to paramagnetic impurities with an isotropic Curie-Weiss susceptibility (Ref. 14) $\chi^{\rm imp}(T)=C/(T-\theta)$, where $C=3.1\times10^{-4}$ K cm^3/mole and $\theta=-0.5$ K. The value of C is equivalent to that of 39 at. ppm of Gd impurities with respect to Y. We partition the measured susceptibility χ as

$$\chi=\chi^{\rm imp}+\chi^{\rm core}+\chi^{\rm Landau}+\chi^{\rm VV}+\chi^{\rm sp}, \qquad (1)$$

where $\chi^{\rm core}$ and $\chi^{\rm Landau}$ are respectively the diamagnetic atomic electron core and Landau conduction-electron orbital susceptibilities, and $\chi^{\rm VV}$ and $\chi^{\rm sp}$ are respectively the paramagnetic Van Vleck orbital and Pauli spin susceptibilities.

To evaluate the $\chi(T)$ data, we calculated the electronic band structure of YNi_2B_2C using the scalar-relativistic, tight-binding, atomic-sphere-approximation, linear-muffin-tin orbital method.[15] The exchange-correlation effects were included within the local density approximation. The bare density of states at the Fermi energy is found to be $N(E_F)=3.95$ states/eV f.u. ("f.u." means formula unit of YNi_2B_2C). We then calculated the Van Vleck susceptibilities ($\chi^{\rm VV,cal}$) versus T, shown in Fig. 1(b), where the isotropic $\chi^{\rm imp}(T)$ from above is also included.

We now test the $\chi(T)$ data in Fig. 1(a) for consistency with band theory. The value of the isotropic, T-independent $\chi^{\rm core}$ term is obtained by summing the values for the constituent Y, Ni, B, and C atoms appropriate to a metallic compound,[13] yielding $\chi^{\rm core}=-1.52\times10^{-4}$ cm^3/mole. The $\chi^{\rm Landau}$ is small in transition metal compounds, comparable to the uncertainty in $\chi^{\rm core}$, and will be neglected. We estimate $\chi^{\rm sp}(T)$ by subtracting the other terms on the right-hand side of Eq. (1), including $\chi^{\rm VV,cal}$, from the measured $\chi(T)$ and the results are shown in Fig. 1(b). The decrease of $\chi^{\rm sp}$ with increasing T is consistent with our band-structure calculations, as follows. Band theory predicts that for $k_BT\ll E_F$, the bare spin susceptibility is[16]

$$\chi^{\rm sp,cal}(T)=\chi^{\rm sp,cal}(0)\left\{1-\frac{\pi^2}{6}\left[\frac{k_BT}{N(E_F)}\right]^2\times[(N'(E_F))^2-N''(E_F)N(E_F)]\right\}, \qquad (2)$$

where the bare $\chi^{\rm sp,cal}(0)=\mu_B^2N(E_F)=1.26\times10^{-4}$ cm^3/mole, which assumes that the conduction-electron gyromagnetic factor $g=2$. The energy derivatives of $N(E)$ at E_F from our band calculations are $N'(E_F)=18.5$ states/(eV)^2 f.u. and $N''(E_F)=-293$ states/(eV)^3 f.u. These values and Eq. (2) yield $\chi^{\rm sp,cal}(T)$ as shown in Fig. 1(b), where the predicted $\chi^{\rm sp,cal}$ is seen to decrease with T, as observed in the $\chi^{\rm sp}(T)$ derived from the data. The average spin susceptibility extrapolated to $T=0$ is $\chi^{\rm sp}_{\rm iso}\equiv(\chi^{\rm sp}_{\|}+2\chi^{\rm sp}_{\perp})/3=1.93\times10^{-4}$ cm^3/mole. The ratio of the experimental to bare band values is $F=1.5$, which should be the same as the Stoner exchange enhancement factor $(1-\alpha)^{-1}$ of the spin susceptibility. Our value $F=1.5$ is indeed comparable with the values of $(1-\alpha)^{-1}$ calculated from band theory for YNi_2B_2C [1.82 (Ref. 6)] and $LuNi_2B_2C$ [1.3$\pm$0.2 (Ref. 4)]. The anisotropy in $\chi^{\rm sp}$ in Fig. 1(b) presumably arises from anisotropy in the g factor, for which band calculations are not available. AF correlations would be expected to suppress $\chi^{\rm sp}$. We conclude that the $\chi(T)$ data are consistent with existing band theory for YNi_2B_2C and, therefore, that our $\chi(T)$ data give no evidence for AF correlations in this compound.

Turning now to our ^{11}B NMR measurements of YNi_2B_2C, the $T_1^{-1}(T)$ results for $H=8.2$ T are shown in

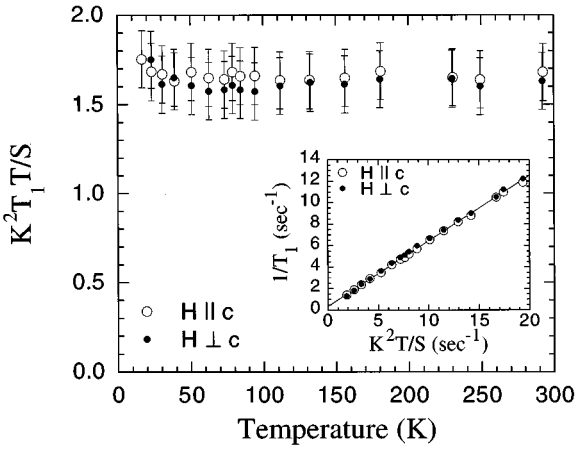

FIG. 3. Korringa ratio $\kappa \equiv K^2T_1T/S$ vs T, where $K \equiv {}^{11}K_{\rm iso}$. The T_1 data are corrected for the paramagnetic impurity contribution $(1/T_1)^{\rm imp} = 0.38$ sec^{-1} from the inset. Inset: ^{11}B T_1^{-1} for $\boldsymbol{H} \| c$ and $\boldsymbol{H} \perp c$ vs K^2T/S. The line is the linear fit $1/T_1 = 0.38$ sec$^{-1} + 0.61(K^2T/S)$ to all of the $1/T_1$ data.

Fig. 2(a); the results are independent of H down to 1.2 T (not shown). The ratio $1/T_1T$ is seen to decrease by about a factor of 2 as T increases from 20 to 300 K, in agreement with previous results.[8–11] No anisotropy of the NSLR is observed within our precision. The measured shifts $^{11}K(T)$, corrected for second order quadrupolar and demagnetization effects, are shown in Fig. 2(b). The anisotropic (axial) part of the shift $K_{\rm ax} \equiv (K_\| - K_\perp)/3$ is more than an order of magnitude smaller than the isotropic part $K_{\rm iso} \equiv (K_\| + 2K_\perp)/3$, as shown in Fig. 2(c), and the latter displays a decrease with T similar to those of $1/T_1T$ and χ above. Since there are no d electrons at the boron site,[6] one can neglect any contribution to K from core polarization and $\chi^{\rm VV}$.[13] Thus we can write

$$K_{\rm iso}(T) = A_s^{\rm at}\chi_s^{\rm sp}(T), \tag{3}$$

where $\chi_s^{\rm sp}(T)$ is the spin susceptibility contribution of the boron $2s$-band electrons at the Fermi surface. Using the $K_{\rm iso}(T)$ data from Fig. 2(c) and the atomic B contact hyperfine constant $A_s^{\rm at} = 1.0 \times 10^6$ G/$N_A\mu_B = 179$ mole B/cm^3,[13] Eq. (3) yields $\chi_s^{\rm sp}(20\ {\rm K}) = 3.0 \times 10^{-6}$ cm^3/mole B. The ratio of this $\chi_s^{\rm sp}$ to the total $\chi_{\rm iso}^{\rm sp}$ from Fig. 1(b) is $r = \chi_s^{\rm sp}(20\ {\rm K})/\chi_{\rm iso}^{\rm sp}(20\ {\rm K}) = 0.015$ which compares well with the corresponding band-structure result (Ref. 6) $r = N_s(E_F)/N(E_F) = 0.04/4.03 = 0.01$, where $N_s(E_F)$ is the s-electron density of states at E_F at the boron site. Thus, the ^{11}K probes only the local $N_s(E_F)$ at the B site and, in particular, not the d-band contribution of the Ni atoms to $N(E_F)$. The large T-dependence of $\chi_s^{\rm sp}(T)$ which can be seen from Eq. (3) and the $K_{\rm iso}(T)$ data in Fig. 2(c) is evidently a consequence of a strongly varying $N_s(E)$ near E_F. The $K_{\rm iso}(T)$ for ^{11}B in YNi_2B_2C can be compared and contrasted with that in $LuRh_4B_4$.[18] In $LuRh_4B_4$, the ^{11}B shift is independent of T in spite of the significant T dependence of χ, implying (i) no coupling of the ^{11}B nuclei with d electrons, consistent with our Eq. (3) for YNi_2B_2C, and (ii) a T-independent $\chi_s^{\rm sp}$, which contrasts with our T-dependent $\chi_s^{\rm sp}$ inferred above for YNi_2B_2C.

The same contact hyperfine interaction in Eq. (3) which is responsible for $^{11}K(T)$ is also responsible for the $T_1^{-1}(T)$, according to the Korringa relation $1/T_1T \propto K^2$.[13] To test this relation, T_1^{-1} versus K^2T/S is plotted in Fig. 3 inset, where for the ^{11}B nucleus $S = (\gamma_e/\gamma_n)^2 h/8\pi^2 k_B = 2.55 \times 10^{-6}$ sec K, and $K(T) \equiv K_{\rm iso}(T)$ based on the fact that the T_1^{-1} data for the two field orientations in Fig. 2(a) are the same within experimental error. The very good linear fit to the data in Fig. 3 inset indicates that there is indeed a predominant Korringa contribution of $1/T_1$. The small y intercept of the fit is ascribed to a small T-independent contribution $(T_1^{-1})^{\rm imp}$ to T_1^{-1} from the paramagnetic impurities detected in the above $\chi(T)$ and in ^{11}B NMR linewidth[17] measurements. The $(T_1^{-1})^{\rm imp} = 0.38$ sec^{-1} found here is of the same order of magnitude (after normalization for the different nuclear gyromagnetic ratios) as the contribution to the proton NSLR in metal hydrides containing $\sim$100 ppm of Gd impurities,[19] which in turn is comparable to the equivalent of 39 at. ppm of Gd impurities giving rise to the $\chi^{\rm imp}(T)$ discussed above.

After subtracting $(T_1^{-1})^{\rm imp}$ from the measured T_1^{-1}, the Korringa ratio $\kappa \equiv K^2T_1T/S$ is plotted in Fig. 3. One expects $\kappa = 1$ for a Fermi gas,[13] whereas $\kappa \cong (1-\alpha)^{-1}$ in the presence of exchange enhancement of $\chi^{\rm sp}$.[20] From Fig. 3 we find a T-independent $\kappa = 1.6 \pm 0.2$, in good agreement with the value $(1-\alpha)^{-1} = F = 1.5$ obtained above from the analysis of $\chi(T)$. We conclude that the decrease of $1/T_1T$ with T in Fig. 2(a) and also observed in Refs. 8–11 for ^{11}B in YNi_2B_2C is simply a reflection of the decrease in $\chi_s^{\rm sp}$ and therefore in $K_{\rm iso}$ with T, which in turn arise from sharp features in $N_s(E)$ near E_F in YNi_2B_2C, a band-structure effect. Thus, one does not need to invoke AF correlations to explain the $(T_1T)^{-1}(T)$ data. From the above, we also infer that the nonlinearity in the $1/T_1T$ vs K^2 plot in Ref. 9 is due to paramagnetic impurities and not to AF correlations as suggested.

We concluded above that $(T_1T)^{-1}(T)$ and $K(T)$ for the ^{11}B NMR are both driven by the same contact hyperfine interaction with the conduction s electrons at the B site and that these data are consistent with band theory. On the other hand, one could argue that since these measurements are only sampling the s electrons at the B site, they may not be sensitive to AF correlations among the d electrons associated with the Ni sublattice. This issue is difficult to address quantitatively in the absence of a specific model and parameters. We limit ourselves to note that the ^{11}B nucleus in YNi_2B_2C occupies a site symmetry where AF correlations of local Ni moments coupled by the dipolar interaction to the ^{11}B nucleus would not be filtered out, whereas indirect exchange coupling would cancel for commensurate AF correlations but not for incommensurate correlations. For the least favorable case of detecting commensurate correlations, one would still observe the contribution to T_1^{-1} due to dipolar coupling.

Finally, we note that $\chi^{\rm imp}(T)$ could not arise from a small magnetic moment localized at each Ni site. In that case, one

would not expect an extra broadening of the line, contrary to our results.[17] One would also expect a T-dependent ($\sim 1/T$) dipolar contribution to $^{11}K_{ax}$ but not to $^{11}K_{iso}$, due to the powder average of the local dipolar field at the B site, again contrary to our observation that $^{11}K_{ax}$ scales linearly with $^{11}K_{iso}$ over the entire T range 16–300 K of our measurements (not shown).

In summary, from the consistency of both the χ and NMR data with band theory, we conclude that no antiferromagnetic correlations or local magnetic moments of nickel are present in YNi_2B_2C.

Ames Laboratory is operated for the U.S. Department of Energy by Iowa State University under Contract No. W-7405-Eng-82. The work at Ames was supported by the Director for Energy Research, Office of Basic Energy Sciences.

*Also at Dipartimento di Fisica, Università di Pavia, 27100 Pavia, Italy.

†Present address: Department of Chemistry, Cornell University, Ithaca, NY 14853.

‡Present address: Department of Physics, College of Natural Science, Hoseo University, Asan, 336-795 Choongnam, Korea.

[1] R. J. Cava *et al.*, Nature **367**, 252 (1994).

[2] T. Siegrist *et al.*, Nature **367**, 254 (1994).

[3] L. F. Mattheiss, Phys. Rev. B **49**, 13 279 (1994).

[4] W. E. Pickett and D. J. Singh, Phys. Rev. Lett. **72**, 3702 (1994).

[5] R. Coehoorn, Physica C **228**, 331 (1994).

[6] J. I. Lee *et al.*, Phys. Rev. B **50**, 4030 (1994).

[7] H. Kim, C-D. Hwang, and J. Ihm, Phys. Rev. B **52**, 4592 (1995).

[8] F. Borsa *et al.*, Physica C **235-240**, 2547 (1994).

[9] K. Ikushima *et al.*, J. Phys. Soc. Jpn. **63**, 2878 (1994).

[10] M. E. Hanson *et al.*, Phys. Rev. B **51**, 674 (1995).

[11] T. Kohara *et al.*, Phys. Rev. B **51**, 3985 (1995).

[12] B. K. Cho *et al.*, Phys. Rev. B **52**, 3684 (1995).

[13] G. C. Carter, L. H. Bennett, and D. J. Kahan, *Metallic Shifts in NMR* (Pergamon, New York, 1977), Pt. I.

[14] Above 100 K, we find $\chi_{iso}=P\chi_{ax}+Q$. Below 50 K, we take the intrinsic χ_{iso} to be $\chi_{iso}^{intr}(T)=P\chi_{ax}(T)+Q$, since χ^{imp} does not contribute to χ_{ax}. Then $\chi^{imp}(T)=\chi_{iso}(T)-\chi_{iso}^{intr}(T)$, which is found to accurately follow a Curie-Weiss law below 50 K.

[15] J. Y. Rhee, X. Wang, and B. N. Harmon, Phys. Rev. B **51**, 15 585 (1995).

[16] N. W. Ashcroft and N. D. Mermin, *Solid State Physics* (Holt, Rinehart and Winston, New York, 1976), p. 669.

[17] An increase in the (≈isotropic) linewidth from ≈6 kHz at 100 K to ≈7.5 kHz at 16 K was observed, attributable to the randomly distributed paramagnetic impurities.

[18] D. C. Johnston and B. G. Silbernagel, Phys. Rev. B **21**, 4996 (1980).

[19] T. T. Phua *et al.*, Phys. Rev. B **28**, 6227 (1983).

[20] R. W. Shaw and W. W. Warren, Phys. Rev. B **3**, 1562 (1971).